

# Jet energy loss due to multiple scattering in the nucleus

M.Braun

Department of high-energy physics,  
University of S. Petersburg, 198904 S. Petersburg, Russia

July 2009

## Abstract

Energy loss of a jet due to multiple collisions in the nuclear target is studied in the framework of the perturbative QCD with an infrared cutoff. An iterational procedure for its calculation is developed, which allows to reliably find up to 16 successive collisions in rescattering. The calculated shift of the scaling variable reaches values of the order 0.1 at medium  $x$  and transverse momentum  $p$  in the interval 5 – 10 GeV/c. The shift is found to be independent of the atomic number of the target and energy.

## 1 Introduction

Jet quenching in nuclear matter due to gluon emission has long been a subject of detailed studies, related to the observed behavior of particle spectra in heavy-ion collisions at RHIC [1]. Much attention has also been devoted to a simpler quenching mechanism due to hard elastic collisions (“collisional quenching”), which is formally of the leading order in  $\alpha_s$  as compared to gluon emission corresponding to inelastic hard collisions. It is expected that quenching due to elastic collisions is proportional to the length  $L$  travelled by the jet inside the nucleus, whereas gluon emission seems to lead to quenching proportional to  $L^2$  [2]. However this conclusion has been derived for superhigh energies. The relative strength the two sources of quenching at present energies is not clear both from the theoretical and experimental points of view [3].

Most calculations of the collisional energy loss (CEL) refer to the propagation of a fast parton in the homogeneous quark-gluon plasma [4, 5, 6, 7]. The study of parton energy loss in a realistic nucleus is a harder task. It requires using the multiple scattering formalism beyond the leading Glauber approximation with full attention to the interplay between the longitudinal and transverse momenta. First calculations made in [8] indicated that elastic collisions diminish the jet energy quite considerably, up to 40% at LHC energies. However due to technical difficulties the authors of [8] were able to push their calculations of multiple hard scattering of the jet inside the nucleus only up to the first three collisions. This is quite insufficient even for RHIC energies at which, as our calculation show, at least 6 collisions are to be taken into account. At the LHC energies this number grows to 12. To obtain reasonable results for the overall quenching due to elastic collisions one has to search for methods which allow to study multiple parton collisions with the loss of energy with a reasonable accuracy. This paper presents an iterative approach which seems to give satisfactory results at both the RHIC and RHIC energies.

Our framework follows that of [9, 10, 11] which considers multiple scattering of a parton existing inside the fast projectile long before the actual collision. The scattering itself is due to the QCD perturbative interaction in the lowest order, with a relatively high transferred transverse momentum and a loss of energy determined by the kinematics. Naturally we introduce an infrared cutoff at low transferred momenta (by an effective gluon mass) and our results depend on the value of this cutoff. On physical grounds we choose it to lie in the region of 1.5–2.0 GeV/c. With such values our iterative procedure gives reliable results up to 16 collisions at the LHC energy.

From the start we have to stress that we consider only passage of a jet through the nucleus. The study of its hadronization is postponed for future publications. We study the cross-sections as a function of the transverse momentum  $p$  of the observed jet and its scaling variable  $x$ . For the study of collisional energy loss of a jet due to rescattering in the nucleus use of these variables is natural. Hadronization, necessary to study the observed parton spectra, can be conveniently calculated in these variables. To pass to c.m. rapidities instead of  $x$  one can use the standard relation  $y = \ln(xW/p)$  where  $W$  is the c.m. energy for proton-proton collisions.

The CEL effect was found to be quite noticeable. For values of  $p$  in the interval 5 – 10 GeV/c and  $x$  of order 0.5 the decrease in the scaling variable was calculated to lie in the interval 0.09 – 1.14. However a curious result is that this decrease does not depend on the energy nor on the atomic number of the target. The latter implies that CEL does not depend on the length of the rescattering path inside the nucleus. Cross-sections themselves exhibit more or less the expected behaviour: they fall with the inclusion of CEL. This fall is only weakly energy dependent, so that the general picture at the RHIC and LHC energies remains practically the same. As a curiosity at the RHIC energy we found that the standard nuclear suppression factor  $R_A$  at small values of  $x$  actually grows with the introduction of CEL. This abnormal behaviour however is not seen at higher values of  $x$  nor at the LHC energies.

## 2 Glauber-like parton rescattering.

To formulate our model and have a benchmark for the following calculations we briefly reproduce here the derivation of the inclusive jet production in hadron-nucleus or nucleus-nucleus scattering in the pure Glauber approximation without loss of energy. The details may be found in the original derivation in [11].

We assume the nuclear state  $|A\rangle$  to be a superposition of states with a different number  $n$  of partons, each characterized by its scaling variable  $x$  and impact parameter  $b$  combined into argument  $z = \{x, b\}$ :

$$|A\rangle = \sum_n \int \prod_{i=1}^n d^3 z_i \Psi_{A,n}(z_i) |n, z_i\rangle. \quad (1)$$

If the observed parton originates from the A-nucleus (moving along the z-axis), then the wave function of the latter is for a given  $n$ :

$$\Psi_{A,n}(z_1, z_2, \dots, z_n) = \sqrt{n} \psi(z_1)_\alpha \tilde{\Psi}_{A,n-1}(z_2, \dots, z_n). \quad (2)$$

Here  $\psi_\alpha(z)$  denotes the wave function of the observed parton, and  $\alpha = \{x, p\}$ , where  $x$  and  $p$  - are the scaling variable and transverse momentum respectively.

The inclusive cross-section of parton production at a given impact parameter  $\beta$  for the nucleus-nucleus (AB) collision is given by the following expression

$$\begin{aligned} \frac{d\sigma}{d^2\beta} &= \sum_{nl} n \int dz_1 dz'_1 \psi_\alpha(z'_1) \psi_\alpha^*(z_1) d\tau_A(n-1) d\tau_B(l) \Psi_{A,n-1}^*(z'_1, z_2, :, z_n) \\ &\times \Psi_{A,n-1}(z_1, :, z_n) |\Psi_{B,l}(u_j)|^2 [S_{nl}^*(z'_1, :, z_n | u_1, :, u_l) - 1] [S_{nl}(z_1, :, z_n | u_1, :, u_l) - 1], \end{aligned} \quad (3)$$

where  $d\tau(n)$  is the phase volume for the state with  $n$  partons. This expression contains contributions of both hard and soft parton interactions. The latter interactions are disregarded because they cannot be studied in the perturbative QCD. The contribution of hard collisions is given by the product  $S_{nl}^* \times S_{nl}$ .

Further transformations rely on the assumption of factorization of nuclear S-matrix into a product of elementary S-matrices corresponding to parton-parton interactions, which is the essence of the Glauber model:

$$S_{nl}(z_1, \dots, z_n | u_1, \dots, u_l) = \prod_{i=1}^n \prod_{j=1}^l s_{ij}. \quad (4)$$

Here  $s_{ij}$  is S-matrix for the interaction of parton  $i$  of the A nucleus with parton  $j$  of the B nucleus, while  $u_j$  - refers to parton variables of nucleus B. We assume factorization of parton distributions:

$$|\Psi_{A(B),l}(u_j)|^2 = \frac{1}{l!} e^{-\langle l \rangle} \prod_{j=1}^l \Gamma(u_j), \quad (5)$$

with  $\langle l \rangle = \int d^3u \Gamma_B(u)$  and  $\Gamma_B(u)$  denoting the product of the parton distribution inside the nucleon and nuclear profile function,

$$\Gamma_{A(B)}(u) = T_{A(B)}(c) P_{A(B)}(\omega). \quad (6)$$

As a result, we get the final expression for the inclusive cross-section of jet production in AB collisions with hard rescattering taken into account:

$$(2\pi)^2 \frac{d\sigma_{AB}}{d^2\beta dx d^2p} = \int d^2b d^2r e^{ipr} T_A(b-\beta) P_A(x) e^{-T_B(b)F_B(x,0)} \{e^{T_B(b)F_B(x,r)} - 1\}, \quad (7)$$

where

$$F_B(x, b) = \int \frac{d^2q}{(2\pi)^2} \int d\omega P_B(\omega) I(x, \omega, q) e^{ipb} \quad (8)$$

and  $I(x, \omega, q)$  is the distribution in the transverse momentum  $q$  in the elastic collision of two partons with their scaling variables  $x$  and  $\omega$ .

For hadron-nucleus collisions one has to change  $T$  into  $\delta$ -function and integrate over  $\beta$  to obtain

$$(2\pi)^2 \frac{d\sigma_{hA}}{dx d^2p} = \int d^2b d^2r e^{ipr} P(x) e^{-T_A(b)F_A(x,0)} \{e^{T_A(b)F_A(x,r)} - 1\}, \quad (9)$$

where  $P(x)$  is the parton distribution in the incoming hadron.

### 3 Energy loss in a single elastic parton collision

#### 3.1 Kinematics

Following the picture of multiple parton scattering let an incoming (massless) parton (4-momentum  $p = (p_+, p_-, p_\perp)$ ) scatter on a target parton (4-momentum  $k = (0, k_-, 0)$ ). The final momenta are  $p' = (p'_+, p'_-, p_\perp - q)$  and  $k' = (k'_+, k'_-, q)$  where  $q$  is the transverse part of the transferred momentum. The scaling variables of the initial and final projectile parton are  $x$  and  $x'$ , those of the target parton  $w$  and  $w'$ . The parton collision c.m. energy squared is  $sw$  where  $s$  is the overall c.m. energy squared. The longitudinal momenta conservation gives

$$p'_+ + \frac{q^2}{2k'_-} = p_+, \quad \frac{(p_\perp - q)^2}{2p'_+} + k'_- = \frac{p_\perp^2}{2p_+} + k_-. \quad (10)$$

The energy loss of the incoming jet is determined by the difference

$$\Delta p_+ = p_+ - p'_+ = \frac{q^2}{2k'_-}, \quad (11)$$

which transforms into the corresponding decrease of the jet scaling variable  $x$ .

From Eqs. (1) we conclude

$$2k'_-p'_+ + q^2 = 2k'_-p_+, \quad 2k'_-p'_+ + (p_\perp - q)^2 = 2p'_+ \left( \frac{p_\perp^2}{2p_+} + k_- \right) \quad (12)$$

and thus

$$q^2 - 2k'_-p_+ = (p_\perp - q)^2 - 2p'_+ \left( \frac{p_\perp^2}{2p_+} + k_- \right). \quad (13)$$

This allows to express  $k'_-$  via  $p'_+$ :

$$k'_- = \frac{1}{2p_+} \left[ 2p'_+ \left( \frac{p_\perp^2}{2p_+} + k_- \right) + q^2 - (p_\perp - q)^2 \right] \quad (14)$$

and obtain an equation:

$$\left( \frac{p'_+}{p_+} - 1 \right) \left( 2p'_+ \left( \frac{p_\perp^2}{2p_+} + k_- \right) + q^2 - (p_\perp - q)^2 \right) + q^2 = 0. \quad (15)$$

This is a quadratic equation from which one determines the initial projectile longitudinal momentum  $p_+$  in terms of its final longitudinal momentum and other variables describing the collision:  $w$ ,  $q$  and  $p_\perp$ . Denoting

$$x = \frac{x'}{1 - u} \quad (16)$$

one finds from (15)

$$u = \frac{1}{p_\perp^2} \left\{ p'_+ k_- + \mathbf{p}_\perp \mathbf{q} - \sqrt{(p'_+ k_- + \mathbf{p}_\perp \mathbf{q})^2 - p_\perp^2 q^2} \right\}. \quad (17)$$

For small transferred momenta  $u$  is proportional to  $q^2$  and then

$$u = \frac{q^2}{swx'}, \quad (18)$$

so that

$$x = \frac{x'}{1 - q^2/(swx')} \quad (19)$$

and is independent of  $p_\perp$ , although the latter may be comparatively large as a result of accumulation of several transferred momenta. We use this simplified formula in our calculations.

Note that condition  $0 < x < 1$  leads to the restriction  $q^2 < sw(x' - x'^2)$ , which limits the region of integration in  $q^2$ ,  $x'$  and  $w$ . From this inequality it also follows that in any case  $q^2 < s(x' - x'^2) \leq s/4$ .

### 3.2 Parton-parton cross-section

In principle one should take into account partons of different flavor both in the projectile hadron and target nucleus. Although it is straightforward, it considerably enhances the calculation time. To economize on the latter, following [12], we considered the effective gluon jet defined by the density

$$P(x, Q^2) = g(x, Q^2) + \frac{4}{9} \left( q(x, Q^2) + \bar{q}(x, Q^2) \right), \quad (20)$$

where  $g, q$  and  $\bar{q}$  are the gluon, quark and antiquark densities respectively. Correspondingly for the parton interaction we took the gluon-gluon one with the cross-section, integrated over the target gluon distribution [12]

$$I(x', q) \equiv \frac{(2\pi)^2 x' d\sigma}{dx' d^2q} = (2\pi)^2 \frac{9\alpha_s^2}{2q^4} \int \frac{dw'}{w'} [xG(x)]_{x'+q^2/sw'} [wG(w)]_{w'+q^2/sx} \left(1 - \frac{q^2}{sxx'}\right)^3, \quad (21)$$

Here, according to our notation,  $x$  and  $w$  refer to initial gluons and  $x'$  and  $w'$  refer to final gluons. We pass to the integration over the initial scaling variable of the target

$$I(x', q) = (2\pi)^2 \frac{9\alpha_s^2}{2q^4} \int \frac{dw}{w - q^2/sx'} [xG(x)]_{x'+q^2/sw'} wG(w) \left(1 - \frac{q^2}{sxx'}\right)^3. \quad (22)$$

From (16) and (18) one finds

$$w - q^2/sx' = w(1 - u), \quad 1 - \frac{q^2}{sxx'} = 1 - u + u^2,$$

so that the cross-section becomes

$$\begin{aligned} I(x', q) &= (2\pi)^2 \frac{9\alpha_s^2}{2q^4} \int \frac{dw}{w} xG(x) wG(w) \frac{(1 - a + a^2)^3}{1 - a} \\ &\simeq (2\pi)^2 \frac{9\alpha_s^2}{2q^4} \int \frac{dw}{w} xG(x) wG(w) (1 - u)^2 \end{aligned} \quad (23)$$

where the second approximate form takes into account that  $q^2$  and consequently  $u$  are assumed to be small. The cross section  $I(x', w, q)$  entering our formulas for the  $n$ -fold cross-section is obtained from this one by dropping the partonic distributions and integration over  $w$ .

## 4 Loss of energy

Eqs. (7) or (9) have an obvious physical interpretation. Developing the exponents in powers of  $F$  one gets, say, for hA collisions the expression for the  $n$ -fold rescattering

$$(2\pi)^2 \frac{d\sigma_{hA}^{(n)}}{dx d^2p} = \frac{1}{n!} \int d^2b d^2r e^{i\mathbf{p}\mathbf{r}} P(x) T_A^n(b) \left\{ \left( F_A(x, r) - F_A(0, r) \right)^n - F_A^n(0, r) \right\} \quad (24)$$

At fixed  $r$  one finds the product of  $n$  inclusive cross-sections  $F_A(x, r)$  summed with similar products in which some of the inclusive cross-sections are substituted by the total cross-sections  $F_A(x, 0)$  with a minus sign. The second term in (24) eliminates the product which does not contain inclusive cross-sections at all. In the momentum space the product goes over into a convolution. So physically this term corresponds to a number  $0 < k \leq n$  of consecutive inclusive cross-sections and  $(n - k)$  total cross-sections distributed among these inclusive cross-sections in all possible ways.

This indicates how one can take into account the loss of energy during rescattering. Each inclusive cross-section in our approximation corresponds to the elastic scattering with a change of transverse momentum. If after  $n$  such collisions the observed scaling variable of the jet is  $x$  then before the  $n$ -th elastic collision and so after the  $(n - 1)$ -th collision the jet has its scaling variable  $x_{n-1} > x$ . Similarly before the  $(n - 1)$ -th collision and after the  $(n - 2)$ -th collision the jet has its scaling variable  $x_{n-2} > x_{n-1}$  and so on. In the first elastic collision the scaling variables before and after the collision are  $x_0$  and  $x_1$  respectively. If the loss of energy would be independent of the scaling variable of the target parton  $w$  then this loss would be accounted for by a simple substitution

$$F_A^n(x, r) \rightarrow \prod_{i=1}^n F(x_i, r) \quad (25)$$

where  $x_i$  are the scaling variables of the jet after the  $i$ -th elastic collision with  $x_n = x$  the scaling variables of the observed jet. However, as we have seen, the change in  $x$  in fact depends on  $w$ , so that this substitution has to be done under the sign of the integration over all scaling variables  $w_i$  of the target partons.

Another problem is to distribute the total cross-sections among the elastic ones with correct scaling variables. Obviously the total cross-sections appearing between the  $k$ -th and  $(k + 1)$ -th elastic ones are to depend on  $x_k$ . For instance for  $n = 2$ , with the loss of energy independent of  $w$ , the original Glauber expression

$$F^2(x, r) - 2F(x, r)F(0, r) \quad (26)$$

should be substituted by

$$F(x_1, r)F(x_2, r) - F(x_2, r)F(x_1, 0) - F(x_2, r)F(x_2, 0), \quad x_2 = x \quad (27)$$

However the  $w$ -dependence again requires making this substitution inside the integral over all  $w$ 's.

A convenient way to obtain constructive formulas which take into account the loss of energy is to set up an iteration procedure allowing to find the  $(n + 1)$ -fold rescattering contribution in terms of the  $n$ -fold one.

### 4.1 Iteration procedure

It is more convenient to work directly in the momentum space. Consider a sequence of  $n$  collisions, some elastic and some total. Call the contribution of the amplitude which ends with the  $n$ -th elastic

collision, with nuclear factor separated,  $X_n(x, p)$  where  $x$  and  $p$  are the scaling variable and transverse momentum of the jet. Then the total contribution with any number of elastic collisions after the last inelastic one is

$$Y_n^{tot}(x, p) = \sum_{k=0}^n X_{n-k}(x, p)[- \sigma(x)]^k, \quad (28)$$

where  $\sigma(x)$  is the total cross-section of the projectile parton and by definition

$$X_0(x, p) = (2\pi)^2 \delta^2(p). \quad (29)$$

From (28) a relation follows

$$Y_n^{tot}(x, r) = X_n(x, r) - \sigma(x)Y_{n-1}^{tot}(x, r). \quad (30)$$

Note that  $Y_n^{tot}(x, r)$  includes an improper term corresponding to the case when there are only elastic collisions:

$$T_n^{tot}(x, p) = Y_n(x, p) + [-\sigma(x)]^n (2\pi)^2 \delta^2(p). \quad (31)$$

Here  $Y_n$  is a contribution from  $n$  collisions with at least one inelastic. One easily finds that also

$$Y_n(x, p) = X_n(x, r) - \sigma(x)Y_{n-1}(x, p). \quad (32)$$

Our basic equation connects  $X_n$  with  $Y_{n-1}^{tot}$ . Under the sign of integration over the target scaling variable  $w$  we have just to convolute  $Y_{n-1}^{tot}(x_{n-1}, p)$  with  $F(x_n, p)$  to obtain

$$X_n(x, p) = \int \frac{d^2q}{(2\pi)^2} dw_n P(w) I(q, x, w) Y_{n-1}^{tot}(x_1, p - q). \quad (33)$$

Here  $x$  is the scaling variable of the projectile AFTER the  $n$ -th collision,  $q$  and  $w$  are the transferred momentum and the scaling variable of the target in this last inelastic collision. The scaling variable  $x_1$  is the one BEFORE the  $n$ -th inelastic collision considered as a function of collision variables

$$x_1 = f(q, x, w). \quad (34)$$

It is generally greater than  $x$ , which corresponds to collisional quenching. The explicit expression of function  $f$  is given by (19). The momentum  $p - q$  is the projectile momentum BEFORE the last inelastic collision. With only one elastic collision

$$X_1(x, p) = \int \frac{d^2q}{(2\pi)^2} dw P(w) I(q, x, w) (2\pi)^2 \delta^2(q - p), \quad (35)$$

which corresponds to

$$Y_0^{tot}(x, p) = (2\pi)^2 \delta^2(p) \quad (36)$$

and follows from our assumption that the projectile has no transverse momentum before all collisions.

Separating the improper contribution to  $Y_{n-1}^{tot}$  in (33) we get

$$X_n(x, p) = \int \frac{d^2q}{(2\pi)^2} dw P(w) I(q, x, w) \left\{ Y_{n-1}(x_1, p - q) + \left( -\sigma(x_1) \right)^{n-1} (2\pi)^2 \delta^2(p - q) \right\} \quad (37)$$

and using relation (32) get the final form of the iteration equation

$$Y_n(x, p) = \int \frac{d^2q}{(2\pi)^2} dw P(w) I(q, x, w) \left\{ Y_{n-1}(x_1, p - q) + \left( -\sigma(x_1) \right)^{n-1} (2\pi)^2 \delta^2(p - q) \right\} - \sigma(x) Y_{n-1}(x, p) \quad (38)$$

One starts iterations with

$$Y_0(x, p) = 0 \quad (39)$$

and successively determines  $T_1$ ,  $T_2$  and so on. At fixed  $b$  the final contribution to the inclusive cross-section is obtained as

$$\frac{(2\pi)^2 d\sigma}{dx d^2p d^2b} = P(x) \sum_{k=1} C_A^n T_A^n(b) Y_n(x, p). \quad (40)$$

This iterative procedure can be directly rewritten in the  $r$  space. One obtains

$$Y_n(x, r) = \int \frac{d^2q}{(2\pi)^2} e^{iqr} dw P(w) I(q, x, w) Y_{n-1}(x_1(q, x, w), r) + \int \frac{d^2q}{(2\pi)^2} e^{iqr} dw P(w) I(q, x, w) \left( -\sigma(x_1(q, x, w)) \right)^{n-1} - \sigma(x) Y_{n-1}(x, r). \quad (41)$$

## 4.2 The master equation

Introduce

$$Z_n = C_A^n T_A^n(b) Y_n(x, p) \simeq \frac{1}{n!} (AT_A(b))^n Y_n(x, p) \equiv \frac{1}{n!} \xi^n Y_n(x, p), \quad (42)$$

where we denoted  $\xi = AT_A(b)$ . Obviously

$$\frac{dZ_n}{d\xi} = \frac{1}{(n-1)!} \xi^{n-1} Y_n(x, p). \quad (43)$$

Now take the recurrent relation (38) and multiply it by  $\xi^{n-1}/(n-1)!$  to get

$$\frac{dZ_n}{d\xi} = \int \frac{d^2q}{(2\pi)^2} dw P(w) I(q, x, w) \left\{ Z_{n-1}(x_1, p - q) + \frac{1}{(n-1)!} \left( -\sigma(x_1) \right)^{n-1} (2\pi)^2 \delta^2(p - q) \right\} - \sigma(x) Z_{n-1}(x, p). \quad (44)$$

Summing from  $n = 1$  to  $\infty$  and defining

$$Z(\xi, x, p) = \sum_{n=1}^{\infty} Z_n, \quad (45)$$

so that

$$\frac{(2\pi)^2 d\sigma}{dx d^2p d^2b} = P(x) Z(\xi, x, p), \quad (46)$$

we obtain a master equation for  $Z$

$$\frac{dZ(\xi, x, p)}{d\xi} = \int \frac{d^2q}{(2\pi)^2} dw P(w) I(q, x, w) \left\{ Z(\xi, x_1, p - q) \right.$$



$$+e^{-\xi\sigma(x_1)}(2\pi)^2\delta^2(p-q)\} - \sigma(x)Z(\xi, x, p). \quad (47)$$

Technically this equation does not present serious advantage as compared to the direct iteration procedure, since it allows to calculate the contribution only at fixed impact parameter  $b$  and requires subsequent integration over  $b$ , which for a fixed number of collisions can be done more easily.

## 5 Numerical results

As mentioned, the iteration procedure allows to reliably calculate rescattering contributions up to the 16th successive collision. We choose the gluon mass  $m = 2$  GeV/c as an effective infrared cutoff. So our inclusive cross-sections are meaningful at  $p_{\perp} > 2$  GeV/c. We study hA collisions with gold as a target ( $A = 197$ ). For comparison also the copper target was studied ( $A = 64$ ). The standard parameter  $K$ , which effectively takes into account higher orders in parton scattering cross-sections has been chosen to be 1.5 at the RHIC energies and 1.0 at the LHC energies. For the parton distributions we used the CTEQ6L set [13].

At the RHIC energy ( $\sqrt{s} = 200$  GeV) the rescattering cross-sections fall very rapidly with the number  $n$  of the subsequent collisions and are practically zero at  $n > 6$ . In contrast at the LHC energy ( $\sqrt{s} = 8800$  GeV) the decrease of the cross-sections with  $n$  is much slower and even the 12th collision contributes  $2 \div 5\%$  of the total cross-section.

Our results for the RHIC energy are presented in Figs. 1-6. In Fig. 1 we illustrate the effect of collisional energy loss (CEL) presenting the ratio of the cross-section with and without CEL

$$Q(x, p) = \frac{d\sigma_A}{dx d^2p} / \left( \frac{d\sigma_A}{dx d^2p} \right)_{no \ energy \ loss} \quad (48)$$

(In the cross-section with no energy loss  $x$  is conserved during rescattering and is equal to  $x$  of the observed jet). As we observe the rate of CEL grows both with  $x$  and  $p$ , somewhat flattening at  $p \geq 10$  GeV/c. In Fig. 2 we compare absolute values of the cross-sections with and without CEL as a function of  $x$  at two values of  $p = 5$  and 10 GeV/c of the transverse momentum. These curves serve us to crudely determine the magnitude of the energy loss  $\Delta$  as a difference between the values of  $x$  at which cross-sections with and without energy loss give the same cross-section. Thus found values of  $\Delta$  are presented in Fig. 3 as a function of  $x$ <sup>1</sup>. They show a maximum at medium values of  $x \sim 0.5$  with  $\Delta = 0.09$  for  $p = 5$  and 0.14 for  $p = 10$ . The growth of collision loss with  $p$  was to be expected from Eq. (19).

An unexpected feature of the CEL is its practical independence of the atomic number of the target. In Fig. 4 we compare the shift  $\Delta$  of the scaling variable for Au and Cu at  $p = 5$  GeV/c. The two curves practically coincide. In the common language it implies that the energy loss does not depend on the length of the path inside the nucleus at all. This can be understood by the fact that the optimal configuration of rescattering to give the observed transverse momentum is to produce this momentum in just one collision, leaving the rest collisions to have a small momentum transfer. Then obviously it does not matter how many scattering centers there are along the rescattering path.

Finally in Figs. 5 and 6 we show the nuclear suppression factor (NSF)

$$R_A(x, p) = \frac{d\sigma_A/(dx d^2p)}{Ad\sigma_1/(dx d^2p)} \quad (49)$$

---

<sup>1</sup>The chosen primitive procedure to find  $\Delta$  fails at high values of  $x$  where the cross-sections become very small, which explains irregularities of the curves at the right end.

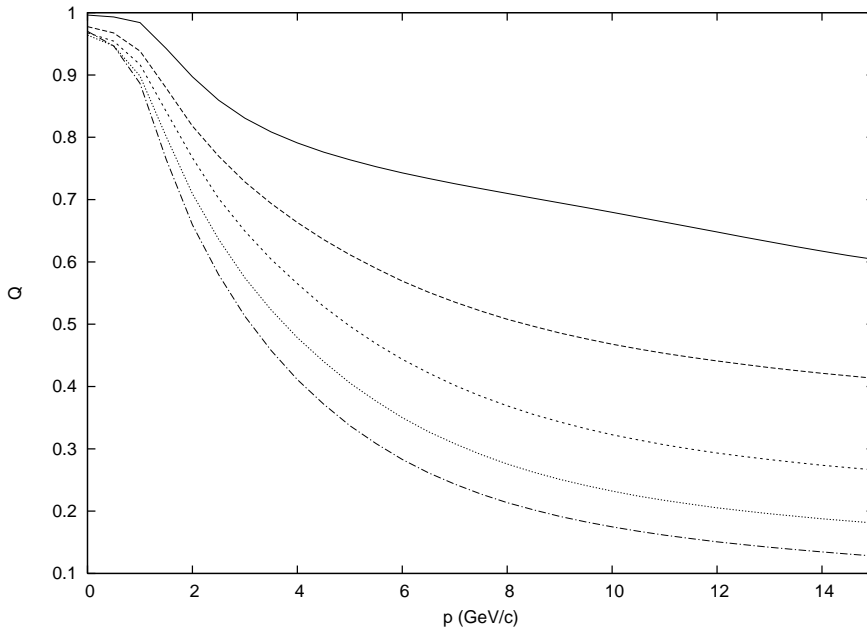


Figure 1: The ratio of the cross-sections with collisional energy loss to the ones without it (Eq. 48) for p-Au collisions at  $\sqrt{s} = 200$  GeV. The curves from top to bottom correspond to  $x = 0.025, 0.2, 0.4, 0.6$  and  $0.8$ .

as a function of  $p$  two values of  $x = 0.025$  and  $0.4$  with and without CEL. The curious result is at low values of  $x$  introduction of CEL actually enhances the NSF ('antiquenching effect'). This is partially the result of the above mentioned optimal configuration for rescattering in which the effect of energy loss may be stronger for the single rescattering contribution than for the total one.

Our results for the LHC energy  $\sqrt{s} = 8800$  GeV and Au target are presented in Figs. 7- 10. Fig. 7 illustrates the CEL showing ratio  $Q(x, p)$  (Eq. (48)) as a function of  $p$  at different values of  $x$ . The general picture remains the same as at the RHIC energy (cf. Fig. 1). However the  $x$  dependence becomes stronger, so that quenching at low  $x$  becomes weaker and at larger  $x$  the same or even stronger. In Fig. 8 we compare the shift  $\Delta$  of the scaling variable at  $p = 5$  GeV/c at LHC and RHIC energies. There is practically no change at all, so that according to our calculations CEL not only is  $A$  independent but also energy independent. Finally Figs. 9 and 10 show the NSF as a function of  $p$  at  $x = 0.025$  and  $0.4$  respectively. At  $x = 0.025$  the effect of CEL is much weaker than at the RHIC energy and acquires the expected direction: it lowers the NSF. At  $x = 0.4$  CEL lowers the NSF much stronger than at the RHIC energy.

## 6 Conclusions

We have calculated collisional energy loss of emitted jets due to multiple collisions of partons from the projectile hadron with partons in the target nuclei. Our results indicate that the loss grows with the transverse momentum  $p$  of the observed jet and is maximal at medium values of the scaling variable  $x$ , where the shift in  $x$  reaches values in the interval  $0.09 - 0.14$  for  $p$  varying from 5 to 10 GeV/c. A somewhat unexpected result is that this shift is practically independent on the atomic number of the target nor on the energy, being the same for RHIC and LHC. The  $A$ -independence implies that the

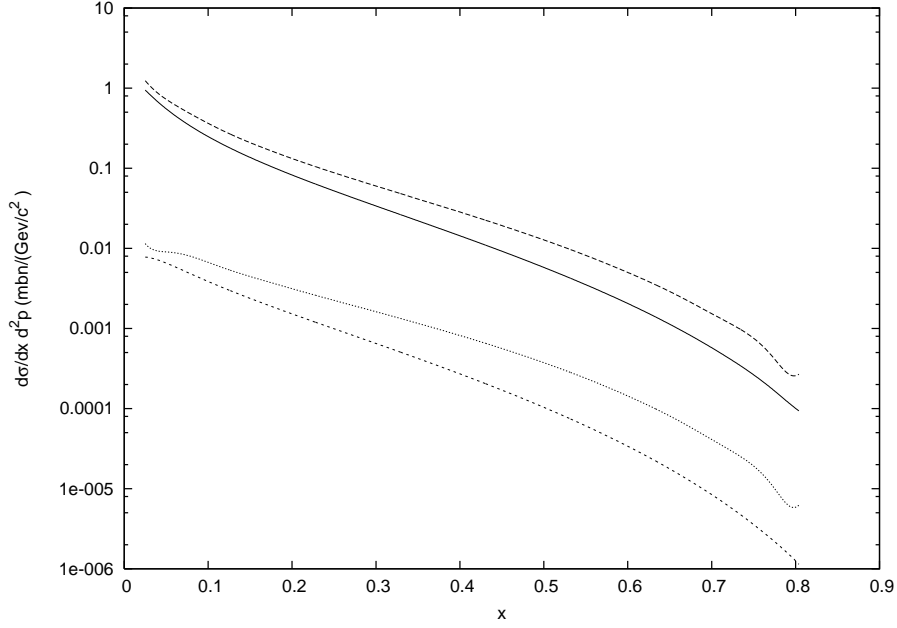


Figure 2: Cross-sections for p-Au collisions at  $\sqrt{s} = 200$  GeV with and without collisional energy loss as a function of  $x$  for  $p = 5$  GeV/c (upper pair of curves) and  $p = 10$  GeV/c (lower pair). In each pair the upper curve corresponds to the absence of energy loss.

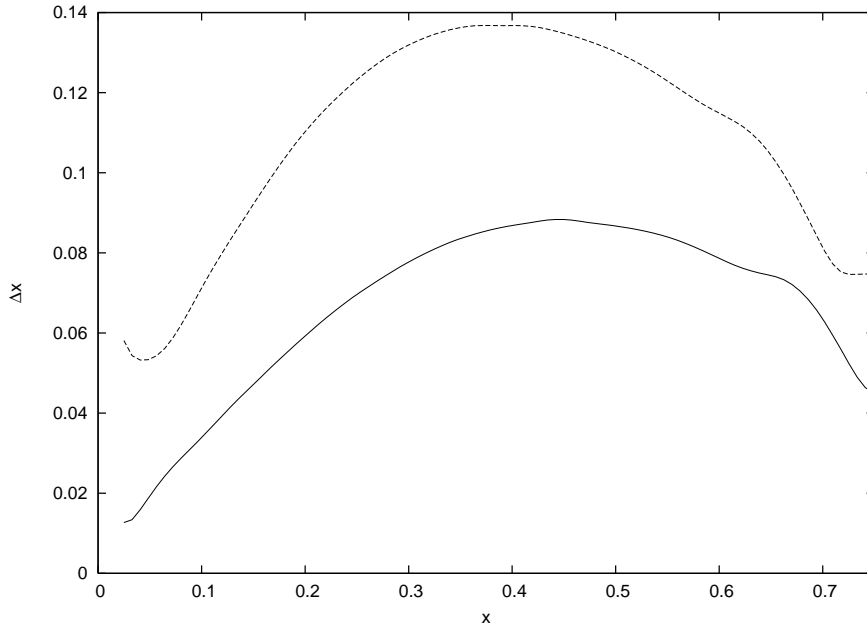


Figure 3: The shift in the scaling variable at  $p = 5$  GeV/c (lower curve) and 10 GeV/c for p-Au collisions at  $\sqrt{s} = 200$  GeV.

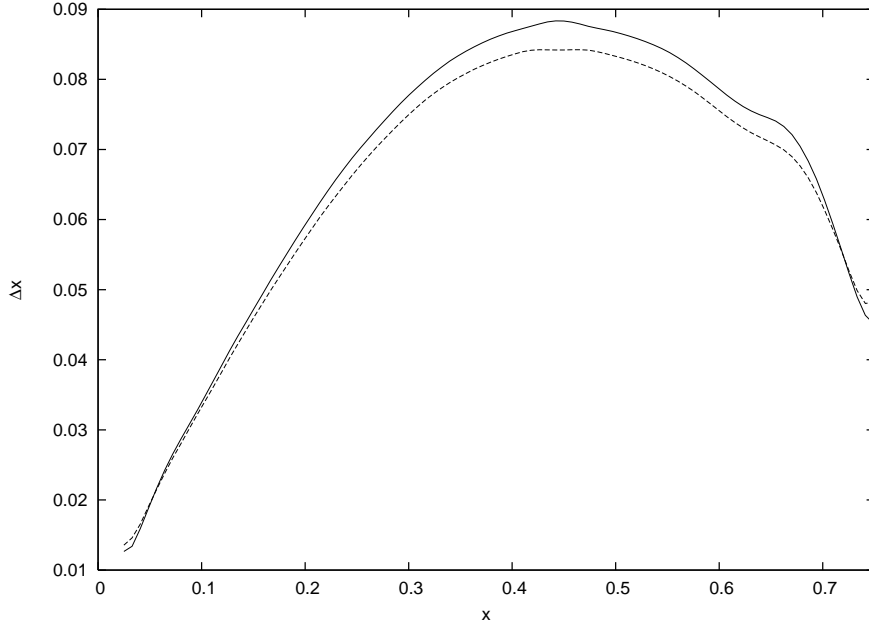


Figure 4: The shift in the scaling variable at  $p = 5$  GeV/c for p-Au (the solid curve) and p-Cu (the dashed curve) collisions at  $\sqrt{s} = 200$  GeV.

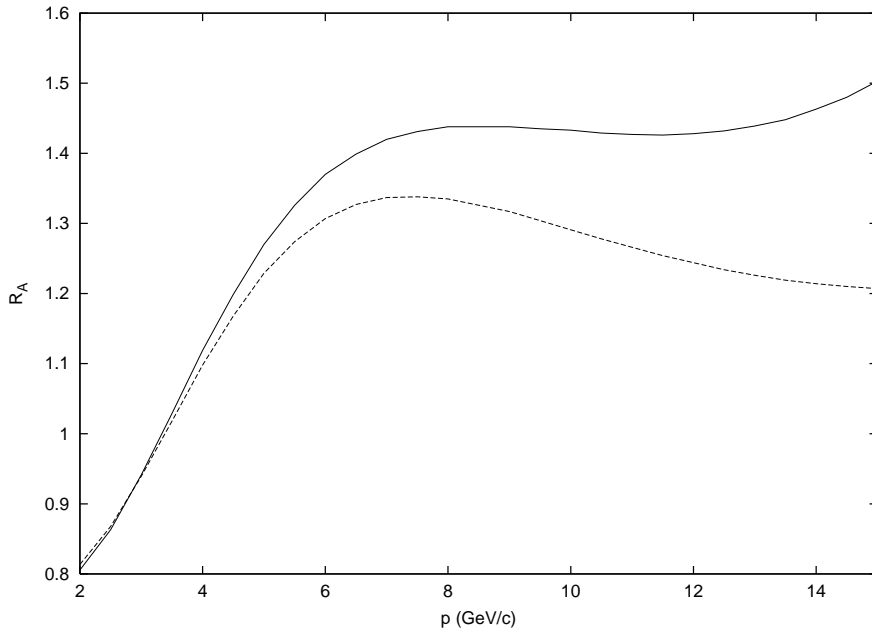


Figure 5: Nuclear suppression factor for p-Au collisions at  $\sqrt{s} = 200$  GeV as a function of transverse momentum  $p$  at  $x = 0.025$  with (the solid curve) and without (the dashed curve) collisional energy loss.

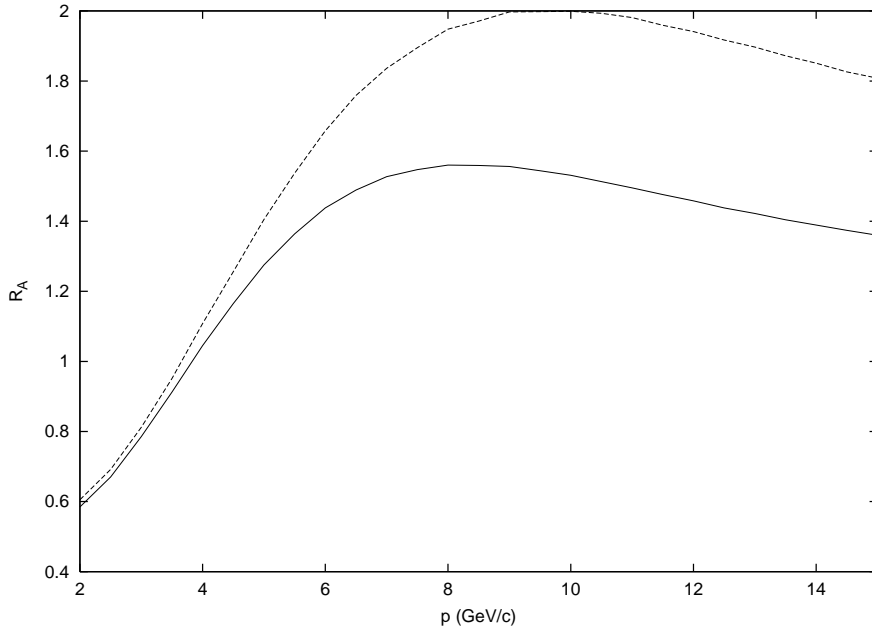


Figure 6: Same as Fig 5 at  $x = 0.4$ .

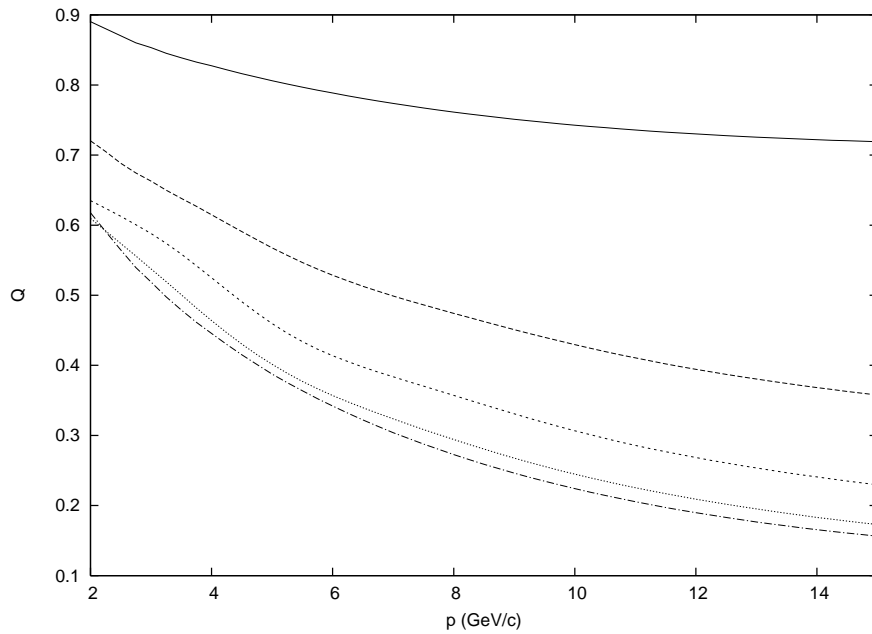


Figure 7: The ratio of the cross-sections with collisional energy loss to the ones without it (Eq. 48) for p-Au collisions at  $\sqrt{s} = 8800$  GeV. The curves from top to bottom correspond to  $x = 0.025, 0.2, 0.4, 0.6$  and  $0.8$ .

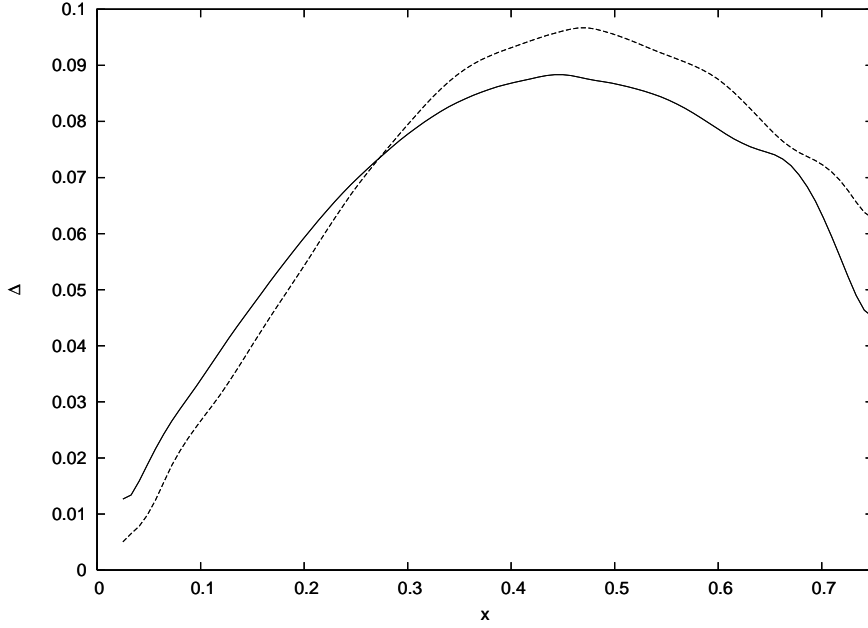


Figure 8: The shift in the scaling variable at  $p = 5$  GeV/c for p-Au collisions at  $\sqrt{s} = 200$  (the solid curve) and 8800 GeV (the dashed curve).

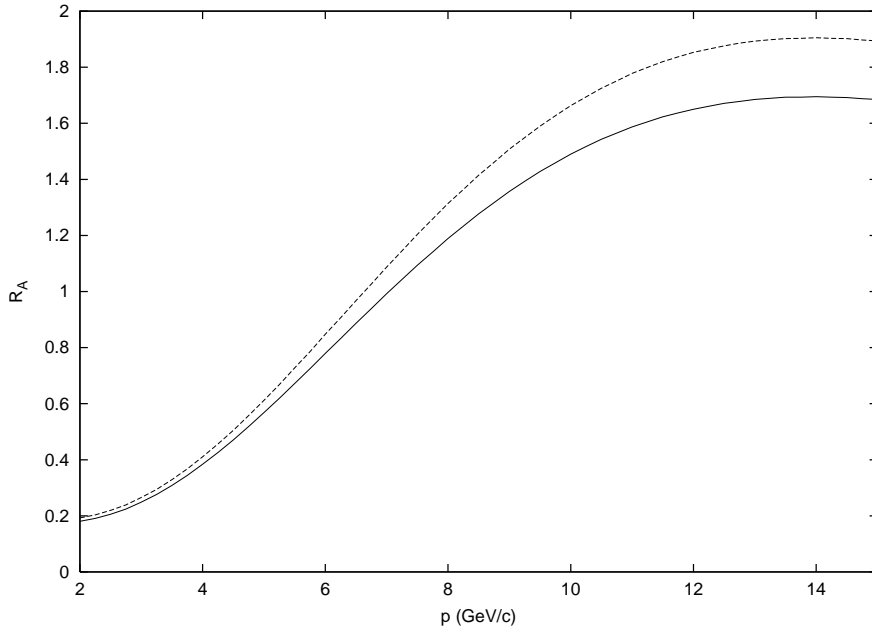


Figure 9: Nuclear suppression factor for p-Au collisions at  $\sqrt{s} = 8800$  GeV as a function of transverse momentum  $p$  at  $x = 0.025$  with (the solid curve) and without (the dashed curve) collisional energy loss

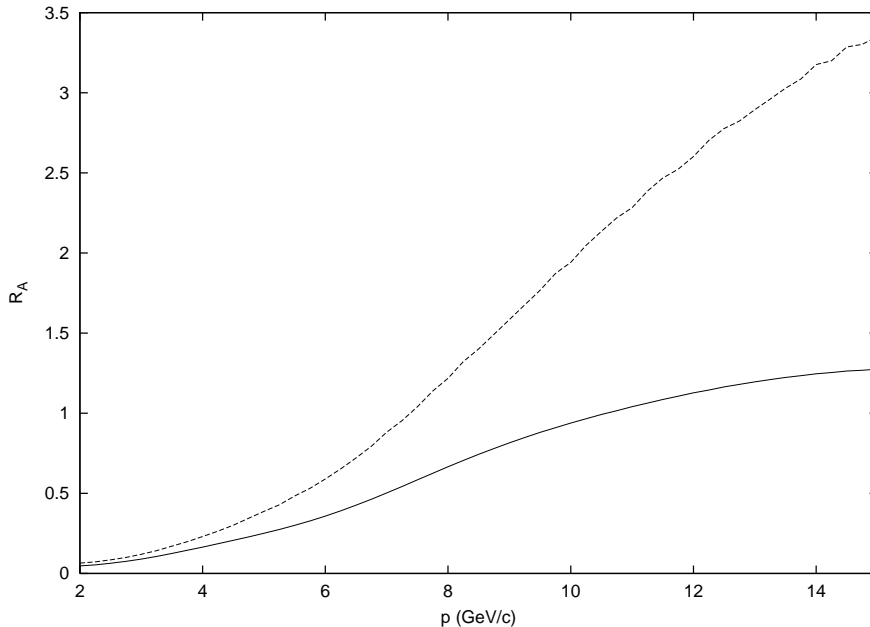


Figure 10: Same as Fig 9 at  $x = 0.4$ .

shift does not depend on the length passed by the jet inside the nucleus. An explanation may be that most of the shift takes place in just one collision during rescattering.

We have also calculated the so-called nuclear suppression factor (NSF) with collisional energy loss taken into account. From our results it follows that at moderate transverse momenta NSF still stays noticeably above unity, indicating that energy loss does not reverse the enhancement in the  $p$ -distribution due to kicks in collisions with partons in the target. Surprisingly at the RHIC energy and small  $x$  the energy loss even enhances NSF, which again may be the consequence that the loss is mostly due to just one collision. However one should take into account that our treatment considers the loss in a single collision to be relatively small, which condition may be violated at small values of  $xs$  (see Eq. (19)).

Finally we stress that our results refer to production of jets. To pass to observed hadrons one should convolute our cross-sections with the appropriate fragmentation functions. Although this procedure seems direct, we prefer to postpone it for future studies, because it inevitably involves new badly controlled assumptions and approximations, especially when hadronization takes place inside the nucleus. We prefer to present results for jets, strictly within the perturbational QCD framework, which do not depend on these soft physics assumptions. They may constitute a starting point for the study of hadronization process.

## 7 Acknowledgments

The author is most grateful to D.Treleani, who initiated the interest of the author in this topic. The author is also very indebted to N.Armesto for constructive discussions, especially concerning literature on the subject. This work has been supported by grants RFFI 09-012-01327-a and RFFI-CERN.

## References

- [1] . J.Casalderrey-Solana and C.A.Salgado, Acta Phys. Polon. **B 38** (2007) 3731 (arXiv:0712.3443).
- [2] R.Baier, Yu.L.Dokshitzer, A.H.Mueller, S. Peigne, D.Schiff, Nucl. Phys. **B 483** (1997) 291.
- [3] N.Armesto, M.Cacciari, A.Dainese, C.A.Salgado, U.A.Wiedemann, Phys. Lett. **B 637** (2006) 362.
- [4] E.Braaten, M.H.Toma Phys. Rev. **D 44** (1991) 1298.
- [5] M.G.Mustafa, Phys. Rev. **C 72** (2005) 014905.
- [6] A.Peshier, Phys. Rev. Lett. **97** (2006) 212301.
- [7] S.Peigne, A.Peshier, Phys. Rev. **D 77** (2008) 114017.
- [8] E.Cattaruzza, D.Treleani, Phys. Rev. **D 69**, (2004) 094006.
- [9] G.Calucci, D.Treleani, Phys. Rev.**D41** (1990) 3367; **D 44** (1991) 2746.
- [10] A.Accardi, D.Treleani, Phys. Rev. **D 64** (2001) 116004.
- [11] M.A.Braun, E.G.Ferreiro, C.Pajares, D.Treleani, Nucl. Phys. **A 723** (2003) 249.
- [12] K.J. Eskola, H.Honkanen, Nucl.Phys. **A 713** (2003) 167.
- [13] J.Pumplin et al., JHEP 0207 (2002) 012.